GPS/INS/Odometer Data Fusion for Land Vehicle Localization in GPS Denied Environment

Mohammed Aftatah[1], Abdelkabir Lahrech[2], Abdelouahed Abounada[1] & Aziz Soulhi[3]

[1] Faculty of Sciences and Techniques, Sultan Moulay Slimane University, Beni Mellal, Morocco

[2] Multidisciplinary Faculty, Hassan First University, Khouribga, Morocco

[3] Superior National School of Mines, Mohamed Fifth University, Rabat, Morocco

Correspondence: Mohammed Aftatah, Faculty of Sciences and Techniques, Sultan Moulay Slimane University, Beni Mellal, Morocco. Tel: 212-0633-249-019. E-mail: mohamed.af5@gmail.com

Abstract

The main purpose of this paper is to present a fusion approach to bridge the period of Global Positioning System (GPS) outages using two proprioceptive sensors that are the Inertial Navigation System (INS) and the odometer in order to assure a continuous localization for land vehicle in urban areas where GPS signal blockage is very often. Odometer and GPS measures are exploited to correct inertial sensor errors. In fact, during GPS availability, INS is integrated with GPS to provide accurate localization solution; whereas during GPS outages, the odometer measurements are used to correct the INS error thereby improving the positioning accuracy and assuring the continuity of navigation solution. The problem of estimation of vehicle localization is realized by Kalman Filter (KF) that merges sensor measurements. The paper thus introduces results from simulation and real data.

Keywords: kalman filtering, Inertial Navigation System, odometer, data fusion, GPS, continuous navigation

1. Introduction

Satellite navigation systems such as GPS or Galileo are increasingly popular and used in strategic as well as public applications. If the safety of persons or property is involved, like in civil aviation, the GPS accuracy is insufficient to be certified as primary means of navigation. One of the solutions is to integrate the GPS with other sensors that provide a good availability such as INS and odometry. Integrated navigation systems have been used intensively in many domains such as aeronautics. However, their application to the automotive industry shows a big increase due to the low cost inertial measurement units (IMU). INS is a system that delivers the position, velocity, and attitude of a vehicle by exploiting the output of inertial sensors. The measurements of the inertial sensors are affected by errors due to physical limitations. The accumulation of these errors leads to the decrease of the accuracy of navigation solution. Therefore, if the error is not compensated with additional sensors, the navigation solution of INS can only be trusted during a short period of time (Seo & Lee, 2005). Nowadays, GPS is very often used as an aiding source to the INS, and the GPS/INS integrated system with good GPS availability provides more precise dynamic positioning than a stand-alone GPS or INS. However, GPS has a low sampling rate thus the satellite signals are not always available due to high buildings, tunnels and mountains, multi-path reflections and bad weather conditions (Noureldin, El-Shafie & Taha, 2007) (Farrell, 1998). To achieve a high level of positioning estimation in an urban area, a new developed integration navigation system is detailed in this paper. Our proposed method is based on the use of an additional aiding source. This additional sensor is the odometer. All modern cars are equipped with the Antilock Braking Systems (ABS) that includes an odometer which measures wheel angular rates and estimate the traveled distance. It is an alternative to satellite-based navigation technology when the GPS measures are not available. The purpose of our work is to propose a global modeling of the GPS/INS/Odometer fusion problem with long GPS outages. The estimation of dynamic characteristics of the vehicle is solved by a KF that fuses the measurements of each sensor to estimate position, velocity and attitude of the vehicle.

This paper traits the performance of the proposed method in terms of accuracy using both simulated and real data. For real tests we have used a Novatel GPS receiver and we estimated the INS and measurements from the real trajectory. In this work additional aiding source information is also considered as an aiding to the positions

delivered by GPS receiver. This extra information is estimated by an odometer. There are four different categories of integration approaches: un-coupled (Titterton & Weston, 1996), loosely coupled (LC) (Wolf, Eissfeller & Hein, 1997) (Solimeno, 2007), tightly coupled (TC) (Li et al., 2006) (Petovello, 2003), and ultra-tightly coupled (UTC) techniques (Babu & Wang, 2007) (Pany, Kaniuth & Eissfeller, 2005) (Petovello & Lachapelle, 2006). The second approach uses GPS and odometer position measurements in addition to the heading angle estimated by the odometery in a Kalman filter that models INS error dynamics. In this paper we have implemented a Loosely Coupled algorithm that has the ability to exploit additional information when available. In such a case, a Kalman filter that uses the position and the heading angle, estimated by the odometer, as measurement has been designed in order to readjust the errors affecting the inertial sensors when GPS signals are absent.

The rest of this paper is organized as follows: Section 2 discusses the INS and the odometer sensor modeling. Section 3 describes the KF fusion algorithm and detailed the system model and the observation model. Section 4 offers simulation results. Finally, section 5 is dedicated to conclusions.

2. Sensors Modeling

2.1 INS Modeling

The equations modeling the INS sensors are used to obtain navigation solutions (position, velocity and orientation of the mobile) from the inertial sensors measurements, i.e. specific forces and angular rates. In this work these equations are expressed in the ENU frame (East, North and Up). In the following the ENU coordinate system will be considered as the navigation frame (n-frame). The body frame (b-frame) is defined at the INS centre. The dynamic equations in the n-frame are given by (Jekeli, 2001) (Abd Rabbou & El-Rabbany, 2015):

$$\dot{r}^{LLa} = DV^n \tag{1}$$

$$\dot{v}^n = C_b^n f_{ib}^b - (2\omega_{ie}^n + \omega_{en}^n) \times v^n + g^n \tag{2}$$

$$\dot{C}_b^n = C_b^n (S(\omega_{nb}^b)) \tag{3}$$

Where $r^n = \begin{bmatrix} \phi & \lambda & \varphi \end{bmatrix}^T$ is the position in the navigation frame, expressed as latitude, longitude and altitude,

$v^n = \begin{bmatrix} v_e & v_n & v_u \end{bmatrix}^T$ is the linear velocity, f_{ib}^b is the specific force measured by accelerometers expressed in the

b-frame, C_b^n is a function of the three orientation angles roll φ, pitch θ and yaw ψ and it's the transformation matrix from the b-frame to the n-frame and vice-versa for C_n^b. ω_{nb}^b is the vector of angular velocities about the axes of the INS provided directly by gyroscopes after removing ω_{ie}^b and ω_{en}^b, ω_{ie}^n is the Earth turn rate in the navigation frame, ω_{en}^n is the turn rate of the n-frame with the respect to the Earth, g^n is the local gravity vector, D is the transformation matrix from the ENU frame to the LLa frame, it's given by (Titterton & Weston, 2004):

$$D = \begin{pmatrix} 0 & \dfrac{1}{R_m + h} & 0 \\ \dfrac{1}{(R_n + h)\cos\phi} & 0 & 0 \\ 0 & 0 & 1 \end{pmatrix} \tag{1a}$$

Where

$$R_m = \frac{a(1-e^2)}{(1-e^2\sin^2\phi)^{3/2}} \tag{1b}$$

$$R_n = \frac{a}{\sqrt{1-e^2\sin^2\phi}} \tag{1c}$$

R_m and R_n are the radii of curvature in the meridian and prime vertical, respectively (Tang et al., 2005). e is the eccentricity of the Earth, a and b are the semi-major axis and semi-minor axis of the Earth, respectively.

(1) Can be expressed in the ENU frame as:

$$\dot{P}^n = V^n \tag{4}$$

Where $P^n = \begin{bmatrix} P_e & P_n & P_u \end{bmatrix}^T$ is the position vector in the navigation frame.

2.2 INS error equations

Eventually, the INS error equations are obtained by perturbing the kinematic equations, i.e. (1-3). These error equations are used in the construction of the GPS/INS/Odometer system model. The perturbation of the position in (1), velocity in (2) and attitude in (3) can be expressed as (5-7), (Angrisano, 2010):

$$\delta\dot{r}^n = F_{rr}\delta r^n + F_{rv}\delta v^n \tag{5}$$

Where

$$F_{rr} = \begin{pmatrix} 0 & 0 & \dfrac{-v_n}{(R_m+h)^2} \\[2ex] \dfrac{v_e \sin\phi}{(R_n+h)\cos^2\phi} & 0 & \dfrac{-v_e}{(R_n+h)\cos\phi} \\[2ex] 0 & 0 & 0 \end{pmatrix} \tag{5a}$$

$$F_{rv} = D \tag{5b}$$

$$\delta\dot{v}^n = F_{vr}\delta r + F_{vv}\delta v + F_{v\epsilon}\epsilon + C_b^n \delta f_{ib}^b \tag{6}$$

Where

$$F_{vr} = \begin{pmatrix} 2\omega_e(v_u\sin\phi + v_n\cos\phi) + \dfrac{v_e v_n}{(R_n+h)\cos^2\phi} & 0 & \dfrac{v_e v_u - v_e v_n \tan\phi}{(R_m+h)^2} \\[2ex] -2\omega_e v_e\cos\phi - \dfrac{v_e^2}{(R_n+h)\cos^2\phi} & 0 & \dfrac{v_n v_u + v_e^2 \tan\phi}{(R_m+h)^2} \\[2ex] -2\omega_e v_e\sin\phi & 0 & \dfrac{-v_e^2}{(R_n+h)} - \dfrac{v_n^2}{(R_m+h)^2} + \dfrac{2g}{R_e+h} \end{pmatrix} \tag{6a}$$

R_e is the radius of the earth and g is the gravity,

$$F_{vv} = \begin{pmatrix} \dfrac{v_n\tan\phi}{R_m+h} - \dfrac{v_u}{R_n+h} & 2\omega_e\sin\phi + \dfrac{v_e\tan\phi}{R_n+h} & -2\omega_e\cos\phi - \dfrac{v_e}{R_n+h} \\[2ex] -2\omega_e\sin\phi - \dfrac{2v_e\tan\phi}{R_n+h} & \dfrac{-v_u}{R_m+h} & \dfrac{-v_n}{R_m+h} \\[2ex] 2\omega_e\cos\phi + \dfrac{2v_e}{R_n+h} & \dfrac{v_n}{R_m+h} & 0 \end{pmatrix} \tag{6b}$$

$$F_{v\epsilon} = \begin{pmatrix} 0 & f_u & -f_n \\ -f_u & 0 & f_e \\ f_n & -f_e & 0 \end{pmatrix} \tag{6c}$$

$f_{ib}^n = \begin{bmatrix} f_e & f_n & f_u \end{bmatrix}^T$ is the specific force in the ENU frame,

$$\dot{\epsilon} = F_{\epsilon r}\delta r^n + F_{\epsilon v}\delta v^n + F_{\epsilon\epsilon}\epsilon + C_b^n \delta\omega_{ib}^b \tag{7}$$

Where

$$F_{\varepsilon r} = \begin{pmatrix} 0 & 0 & \dfrac{-v_n}{(R_m + h)^2} \\ \omega_e \sin\phi & 0 & \dfrac{v_e}{(R_n + h)^2} \\ -\omega_e \cos\phi - \dfrac{v_e}{(R_n + h)\cos^2\phi} & 0 & \dfrac{v_e \tan\phi}{(R_n + h)^2} \end{pmatrix} \tag{7a}$$

$$F_{\varepsilon v} = \begin{pmatrix} 0 & \dfrac{1}{(R_m + h)} & 0 \\ \dfrac{-1}{R_n + h} & 0 & 0 \\ \dfrac{-\tan\phi}{R_m + h} & 0 & 0 \end{pmatrix} \tag{7b}$$

$$F_{\varepsilon\varepsilon} = \begin{pmatrix} 0 & \omega_e \sin\phi + \dfrac{v_e \tan\phi}{R_n + h} & -\omega_e \cos\phi - \dfrac{v_e}{R_n + h} \\ -\omega_e \sin\phi - \dfrac{v_e \tan\phi}{R_n + h} & 0 & \dfrac{-v_n}{R_m + h} \\ \omega_e \cos\phi + \dfrac{v_e}{R_n + h} & \dfrac{v_n}{R_m + h} & 0 \end{pmatrix} \tag{7c}$$

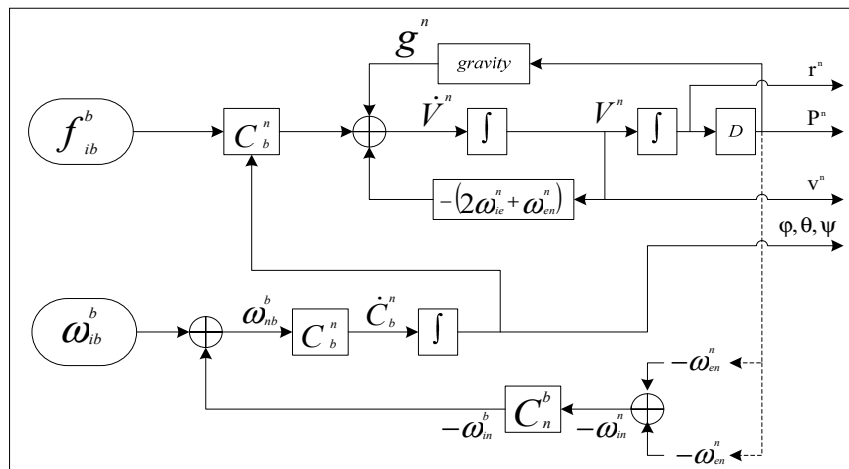The INS mechanization in the navigation frame is summarized in figure 1 as follows:

Figure 1. INS mechanization in ENU frame, adopted from (Schultz, 2006) (Quinchia et al., 2013)

2.3 Odometer Modeling

The kinematic equations of the char vehicle model figured in figure 2 are given by (Abuhadrous, 2005):

$$\begin{cases} u = r_{wheel}\left(\dfrac{\omega_R + \omega_L}{2}\right) \\ \dot{\theta} = r_{wheel}\left(\dfrac{\omega_R - \omega_L}{e}\right) \end{cases} \tag{8}$$

Where ω_R and ω_L are the angular velocities of the right and left wheels, respectively. $\dot{\theta}$ is the heading angle rate

(angular velocity) of the vehicle in the x-y plane, r_{wheel} is the radius of the two wheels, e is the length of the axle of the vehicle (distance between the two wheels), $v_R = r_{wheel}\omega_R$ and $v_L = r_{wheel}\omega_L$ are the velocities of the left and right wheels respectively, u is the average of the two velocities.

The angular velocities or the measured displacements in (8) for the right wheel are written as (Lahrech, Boucher & Noyer, 2005):

$$\omega_{t+1}^R = r_R^{-1}\sqrt{(\omega_{t+1}^{R,x})^2 + (\omega_{t+1}^{R,y})^2} \qquad (9)$$

Where

$$\omega_{t+1}^{R,x} = v_t^x \Delta t + \frac{e}{2}\left(\frac{v_{t+1}^y}{\sqrt{(v_{t+1}^x)^2 + (v_{t+1}^y)^2}} - \frac{v_t^y}{\sqrt{(v_t^x)^2 + (v_t^y)^2}} \right) \qquad (9a)$$

$$\omega_{t+1}^{R,y} = v_t^y \Delta t - \frac{e}{2}\left(\frac{v_{t+1}^x}{\sqrt{(v_{t+1}^x)^2 + (v_{t+1}^y)^2}} - \frac{v_t^x}{\sqrt{(v_t^x)^2 + (v_t^y)^2}} \right) \qquad (9b)$$

And for the left wheel (Lahrech, Boucher & Noyer, 2005):

$$\omega_{t+1}^L = r_L^{-1}\sqrt{(\omega_{t+1}^{L,x})^2 + (\omega_{t+1}^{L,y})^2} \qquad (10)$$

Where

$$\omega_{t+1}^{L,x} = v_t^x \Delta t - \frac{e}{2}\left(\frac{v_{t+1}^y}{\sqrt{(v_{t+1}^x)^2 + (v_{t+1}^y)^2}} - \frac{v_t^y}{\sqrt{(v_t^x)^2 + (v_t^y)^2}} \right) \qquad (10a)$$

$$\omega_{t+1}^{L,y} = v_t^y \Delta t + \frac{e}{2}\left(\frac{v_{t+1}^x}{\sqrt{(v_{t+1}^x)^2 + (v_{t+1}^y)^2}} - \frac{v_t^x}{\sqrt{(v_t^x)^2 + (v_t^y)^2}} \right) \qquad (10b)$$

r_R and r_L are the radii of the right and left wheels respectively, e is the distance separating the two points of contact of the wheels with the ground.
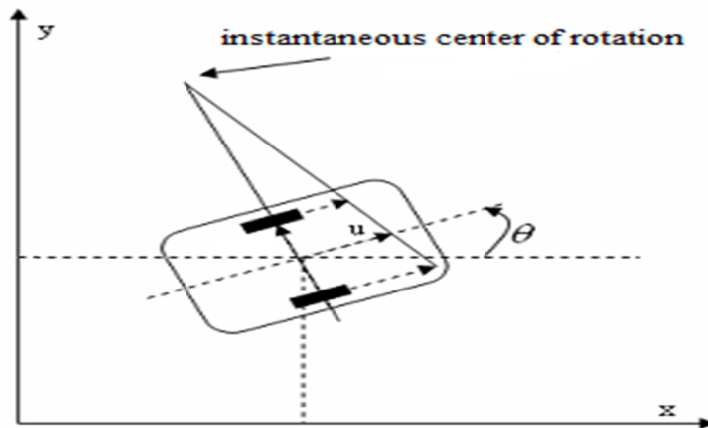

Figure 2. The char vehicle model, kindly taken from (Abuhadrous, 2005)

The odometer measurements are exploited in case of GPS outages. The discrete form of the equations used to obtain position from odometer measures can be expressed as (Abuhadrous, 2005):

$$\begin{cases} x_{k+1} = x_k + (u \cos \theta_{k+1})\Delta t \\ y_{k+1} = y_k + (u \sin \theta_{k+1})\Delta t \\ \theta_{k+1} = \theta_k + \dot{\theta}\Delta t \end{cases} \tag{11}$$

Where x_k and y_k denote the position in the center of the axis, Δt is the sampling time.

3. Kalman Filter Fusion Modeling

A KF is chosen to fuse the measurements of the INS and GPS when sufficient satellite signals are available and to integrate INS measures with odometer in the opposite case. The filter structure is shown in figure 3. The Kalman filter algorithm has two main steps: the first consists in predicting the state based on the system model and the second is dedicated to update the state based on the measurements (Grewal & Andrews, 1993).
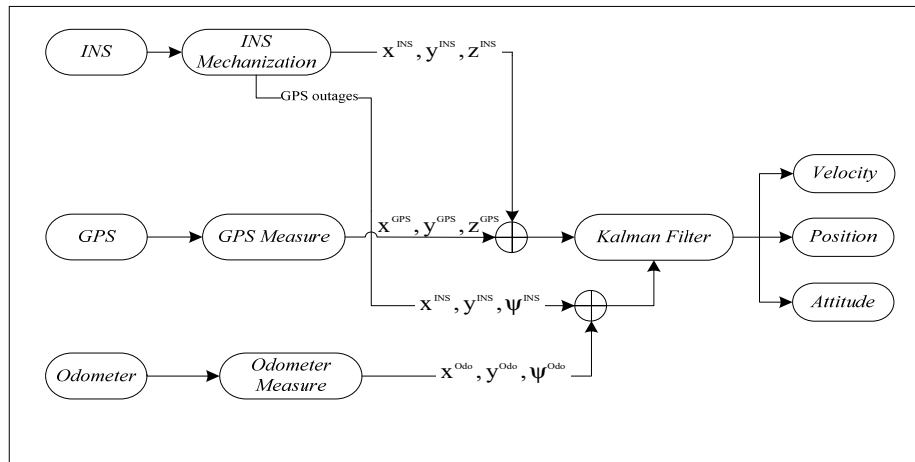

Figure 3. The filter structure

3.1 System Model

The INS error equations are used in the Kalman filter as the system error dynamic model of integrated navigation (Angrisano, 2010):

$$\dot{X} = \begin{pmatrix} \delta\dot{r}^n \\ \delta\dot{v}^n \\ \dot{\varepsilon} \\ \delta\dot{b}_{acc} \\ \delta\dot{b}_{gyro} \end{pmatrix} = \begin{pmatrix} F_{rr} & F_{rv} & 0_3 & 0_3 & 0_3 \\ F_{vr} & F_{vv} & F_{v\varepsilon} & C_b^n & 0_3 \\ F_{\varepsilon r} & F_{\varepsilon v} & F_{\varepsilon\varepsilon} & 0_3 & C_b^n \\ 0_3 & 0_3 & 0_3 & \alpha_{bacc} & 0_3 \\ 0_3 & 0_3 & 0_3 & 0_3 & \alpha_{bgyro} \end{pmatrix} \begin{pmatrix} \delta r^n \\ \delta v^n \\ \varepsilon \\ \delta b_{acc} \\ \delta b_{gyro} \end{pmatrix}$$

$$+ \begin{pmatrix} 0_3 & 0_3 & 0_3 & 0_3 \\ C_b^n & 0_3 & 0_3 & 0_3 \\ 0_3 & C_b^n & 0_3 & 0_3 \\ 0_3 & 0_3 & I_3 & 0_3 \\ 0_3 & 0_3 & 0_3 & I_3 \end{pmatrix} \begin{pmatrix} \eta_{acc} \\ \eta_{gyro} \\ \eta_{bacc} \\ \eta_{bgyro} \end{pmatrix} \tag{12}$$

Where $X = \begin{bmatrix} \delta r^n & \delta v^n & \varepsilon & \delta b_{acc} & \delta b_{gyro} \end{bmatrix}^T$ is the state vector, δr^n is the position errors, δv^n is the linear velocity errors, ε is the Euler angles errors, $\delta b_{acc} = \begin{bmatrix} \delta b_{accx} & \delta b_{accy} & \delta b_{accz} \end{bmatrix}^T$ and $\delta b_{gyro} = \begin{bmatrix} \delta b_{gyrox} & \delta b_{gyroy} & \delta b_{gyroz} \end{bmatrix}^T$ are the biases of accelerometers and gyroscopes, 0_3 and I_3 are zero and identity matrices of size 3, the drift of these biases can be modeled as a first-order Gauss-Markov process (Hou, 2004) represented as follow:

$$\delta\dot{b}_{acci} = \frac{-1}{\tau_{bacci}}\delta b_{acci} + \eta_{bacci} \tag{12a}$$

$$\delta \dot{b}_{gyroi} = \frac{-1}{\tau_{bgyroi}} \delta b_{gyroi} + \eta_{bgyroi} \tag{12b}$$

Where i=x, y, z,

$\frac{-1}{\alpha_{acc}} = \begin{bmatrix} \tau_{baccx} & \tau_{baccy} & \tau_{baccz} \end{bmatrix}^T$ is the correlation times for the accelerometers,

$\frac{-1}{\alpha_{gyro}} = \begin{bmatrix} \tau_{bgyrox} & \tau_{bgyroy} & \tau_{bgyroz} \end{bmatrix}^T$ is the correlation times for the gyroscopes,

$\eta_{acc} = \begin{bmatrix} \eta_{accx} & \eta_{accy} & \eta_{accz} \end{bmatrix}^T$ is the accelerometers noises,

$\eta_{gyro} = \begin{bmatrix} \eta_{gyrox} & \eta_{gyroy} & \eta_{gyroz} \end{bmatrix}^T$ is the gyroscopes noises,

$\eta_{bacc} = \begin{bmatrix} \eta_{baccx} & \eta_{baccy} & \eta_{baccz} \end{bmatrix}^T$ and $\eta_{bgyro} = \begin{bmatrix} \eta_{bgyrox} & \eta_{bgyroy} & \eta_{bgyroz} \end{bmatrix}^T$ are the Gauss-Markov process driving noises,

Because the values of position error in (9) are very small, since they are expressed in radian, and can cause numerical instability inside the filter, to avoid this problem it is better to express the position error in the ENU frame (East, North and Up coordinates) (Shin, 2001), the new dynamic model is :

$$\dot{X} = \begin{pmatrix} \delta \dot{P}^n \\ \delta \dot{v}^n \\ \dot{\varepsilon} \\ \delta \dot{b}_{acc} \\ \delta \dot{b}_{gyro} \end{pmatrix} = \begin{pmatrix} F_{PP} & F_{Pv} & 0_3 & 0_3 & 0_3 \\ F_{vP} & F_{vv} & F_{v\varepsilon} & C_b^n & 0_3 \\ F_{\varepsilon P} & F_{\varepsilon v} & F_{\varepsilon \varepsilon} & 0_3 & C_b^n \\ 0_3 & 0_3 & 0_3 & \alpha_{bacc} & 0_3 \\ 0_3 & 0_3 & 0_3 & 0_3 & \alpha_{bgyro} \end{pmatrix} \begin{pmatrix} \delta P^n \\ \delta v^n \\ \varepsilon \\ \delta b_{acc} \\ \delta b_{gyro} \end{pmatrix}$$
$$+ \begin{pmatrix} 0_3 & 0_3 & 0_3 & 0_3 \\ C_b^n & 0_3 & 0_3 & 0_3 \\ 0_3 & C_b^n & 0_3 & 0_3 \\ 0_3 & 0_3 & I_3 & 0_3 \\ 0_3 & 0_3 & 0_3 & I_3 \end{pmatrix} \begin{pmatrix} \eta_{acc} \\ \eta_{gyro} \\ \eta_{bacc} \\ \eta_{bgyro} \end{pmatrix} \tag{13}$$

Where

$$F_{PP} = \begin{pmatrix} 0 & \dfrac{v_e \tan \phi}{R_m + h} & \dfrac{-v_e}{R_n + h} \\ 0 & 0 & \dfrac{-v_n}{R_m + h} \\ 0 & 0 & 0 \end{pmatrix} \tag{13a}$$

$$F_{Pv} = \begin{bmatrix} 1 & 0 & 0 \\ 0 & 1 & 0 \\ 0 & 0 & 1 \end{bmatrix} \tag{13b}$$

$$F_{vP} = \begin{pmatrix} 0 & \dfrac{2\omega_e(v_u\sin\phi + v_n\cos\phi)}{R_m+h} + \dfrac{v_e v_n}{(R_m+h)(R_n+h)\cos^2\phi} & \dfrac{v_e(v_u - v_n\tan\phi)}{(R_n+h)^2} \\[3mm] 0 & \dfrac{-2\omega_e v_e\cos\phi}{R_m+h} - \dfrac{v_e^2}{(R_m+h)(R_n+h)\cos^2\phi} & \dfrac{-2\omega_e v_e\cos\phi}{R_m+h} - \dfrac{v_e^2}{(R_m+h)(R_n+h)\cos^2\phi} \\[3mm] 0 & \dfrac{-2\omega_e v_e\sin\phi}{R_m+h} & \dfrac{-v_n^2}{(R_m+h)^2} - \dfrac{v_e^2}{(R_n+h)^2} + \dfrac{2g}{R_e+h} \end{pmatrix} \tag{13c}$$

$$F_{\varepsilon P} = \begin{pmatrix} 0 & 0 & \dfrac{-v_n}{(R_m+h)^2} \\[3mm] 0 & \dfrac{\omega_e\sin\phi}{R_m+h} & \dfrac{v_e}{(R_n+h)^2} \\[3mm] 0 & \dfrac{-\omega_e\cos\phi}{R_m+h} - \dfrac{v_e}{(R_m+h)(R_n+h)\cos^2\phi} & \dfrac{v_e\tan\phi}{(R_n+h)^2} \end{pmatrix} \tag{13d}$$

The discrete form of the system model can be written as:

$$X_k = \begin{pmatrix} I_3+F_{pp}\Delta t & F_{pv}\Delta t & 0_3 & 0_3 & 0_3 \\ F_{vp}\Delta t & I_3+F_{vv}\Delta t & F_{v\varepsilon}\Delta t & C_b^n\Delta t & 0_3 \\ F_{\varepsilon P}\Delta t & F_{\varepsilon v}\Delta t & I_3+F_{\varepsilon\varepsilon}\Delta t & 0_3 & C_b^n\Delta t \\ 0_3 & 0_3 & 0_3 & I_3+\alpha_{bacc}\Delta t & 0_3 \\ 0_3 & 0_3 & 0_3 & 0_3 & I_3+\alpha_{bgyro}\Delta t \end{pmatrix}_{k-1} X_{k-1}$$
$$+ \begin{pmatrix} 0_3 & 0_3 & 0_3 & 0_3 \\ C_b^n & 0_3 & 0_3 & 0_3 \\ 0_3 & C_b^n & 0_3 & 0_3 \\ 0_3 & 0_3 & I_3 & 0_3 \\ 0_3 & 0_3 & 0_3 & I_3 \end{pmatrix}_{k-1} \begin{pmatrix} \eta_{acc} \\ \eta_{gyro} \\ \eta_{bacc} \\ \eta_{bgyro} \end{pmatrix}_{k-1} \tag{14}$$

Where Δt is the sampling time.

3.2 Observation Model

3.2.1 GPS Measurements

When the GPS signals are available, position and velocity solution from GPS are integrated with INS at the rate of 1 Hz. The measurement model for GPS/INS loosely coupled scheme is:

$$Z_{GPS} = H_{GPS}.X + \upsilon^{GPS} = \begin{bmatrix} x^{INS} - x^{GPS} \\ y^{INS} - y^{GPS} \\ z^{INS} - z^{GPS} \end{bmatrix} + \upsilon^{GPS} \tag{15}$$

Where $\upsilon^{GPS} \sim \aleph(0, R_{GPS})$ is a white Gaussian noise.

The observation matrix is:

$$H_{GPS} = \begin{bmatrix} 1 & 0 & 0 & 0_{1\times(n-3)} \\ 0 & 1 & 0 & 0_{1\times(n-3)} \\ 0 & 0 & 1 & 0_{1\times(n-3)} \end{bmatrix} \tag{16}$$

Where n is the size of the state vector, $I_{3\times3}$ is the identity matrix, $0_{3\times3}$ is a zero matrix and the subscript $(m\times n)$ shows the number of matrix rows (m) and columns (n). GPS measurements have as covariance matrix:

$$R_{GPS} = \begin{bmatrix} \sigma^2_{x_{GPS}} & 0 & 0 \\ 0 & \sigma^2_{y_{GPS}} & 0 \\ 0 & 0 & \sigma^2_{z_{GPS}} \end{bmatrix} \tag{17}$$

Where $\sigma^2_{P_{GPS}}$ is the covariance of P_{GPS} and P=x, y, z.

3.2.2 Odometer Measurements

In denied environments when GPS signals are not available, position solution from the odometer is integrated with the INS at the rate of 1 Hz. In this case, the measurement model is given by:

$$Z_{Odo} = H_{Odo}.X + \upsilon^{Odo} = \begin{bmatrix} x^{INS} - x^{Odo} \\ y^{INS} - y^{Odo} \\ \psi^{INS} - \psi^{Odo} \end{bmatrix} + \upsilon^{Odo} \tag{18}$$

Where $\upsilon^{Odo} \sim \aleph(0, R_{Odo})$ is a white Gaussian noise.

The observation matrix has the following form:

$$H_{Odo} = \begin{bmatrix} 1 & 0 & 0_{1x6} & 0 & 0_{1x6} \\ 0 & 1 & 0_{1x6} & 0 & 0_{1x6} \\ 0 & 0 & 0_{1x6} & 1 & 0_{1x6} \end{bmatrix} \tag{19}$$

Where n is the size of the state vector.

The covariance matrix of odometer measurements is given by:

$$R_{Odo} = \begin{bmatrix} \sigma^2_{x_{Odo}} & 0 & 0 \\ 0 & \sigma^2_{y_{Odo}} & 0 \\ 0 & 0 & \sigma^2_{\psi_{Odo}} \end{bmatrix} \tag{20}$$

Where $\sigma^2_{P_{Odo}}$ is the covariance of P_{Odo} and P=x, y, z.

4. Simulation Results

The section below is dedicated to present some results from our fusion algorithm applied to simulation data in the purpose to quantify the contribution of the developed solution in terms of accuracy and availability of vehicle positioning in urban areas.

4.1 Simulated Scenario

In the simulated trajectory of the vehicle, during 26 minutes and 37 seconds (figure 4), there are three zones where the GPS signals are not available mainly because of the masking of satellite signals or an insufficient number of visible satellites: the three zones have duration of 70 seconds each. During these periods, the estimator uses the odometer measures in order to correct inertial sensor errors.
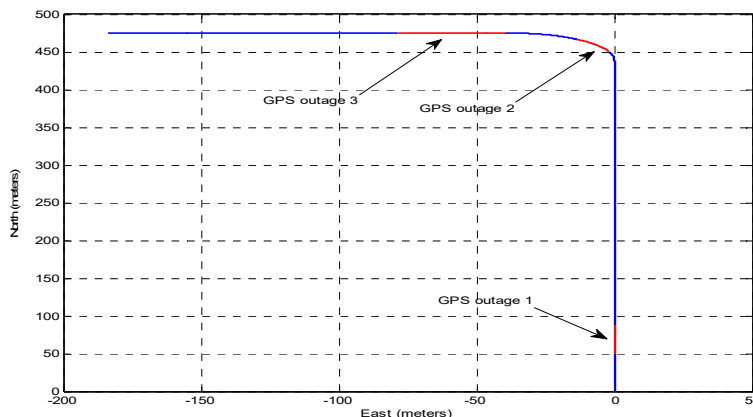
Figure 4. Trajectory taken for simulation including long GPS outages

4.2 Vehicle Localization

Here we present the results from our fusion algorithm applied to simulation data. During the GPS outages, the filter uses the odometer measures to correct the errors affecting the inertial sensors. To calculate the errors the reference trajectory of the vehicle is used.
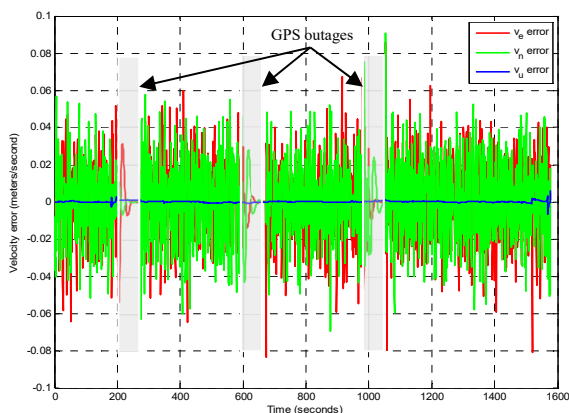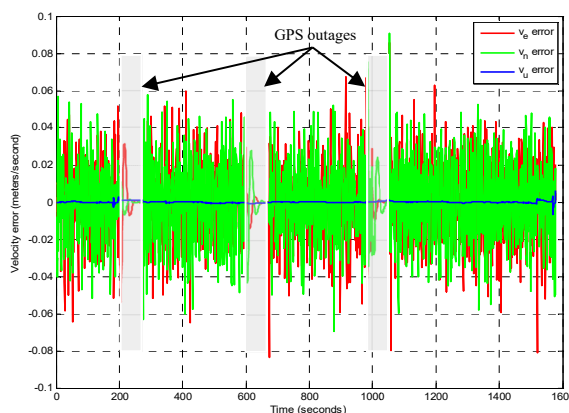

Figure 5. Velocity error of the vehicle
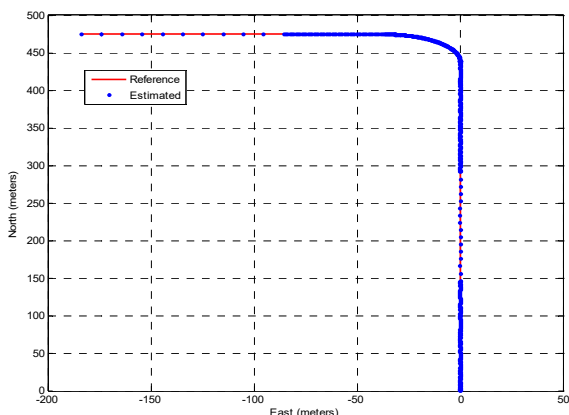

Figure 6. Positioning error of the vehicle

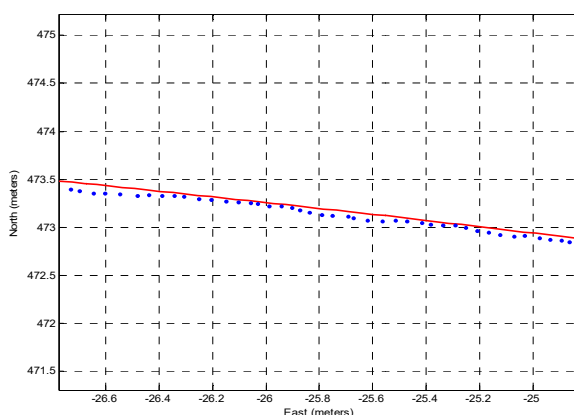Figure 7. Estimated trajectory of the vehicle

Figure 8. Zoom on reference and estimated trajectories

Figure 5 shows the velocity error of the vehicle. We can notice that this error is approximately 0.005

meters/second in the presence of GPS signal blockages. The use of an additional aiding source, the odometer, leads to good results in terms of vehicle velocity estimation. In fact, the estimated error of the vehicle velocity is significantly reduced during GPS signal outages. As shown in figure 6, the proposed method improves significantly the vehicle positioning accuracy even during long GPS outages: the error does not exceed 0.3 meters for the horizontal component and the East and North components. A 2-D plot of the simulated trajectory and the estimated one are show below. It is clear by observing Fig. 7 and Fig. 8 that the position errors of the GPS/INS/Odometer integrated navigation system are smaller than those of GPS/INS integrated navigation system. Especially, where GPS signal is absent. From these results, it can be seen that the proposed algorithm fusion improves the accuracy of vehicle localization. In addition to this, the GPS/INS/Odometer integrated system realized by using the proposed data fusion methodology leads to good performance compared with the GPS/INS integrated system during GPS outages.

4.3 Real Data Test Results

This section is dedicated to the presentation of the results obtained by the application of the new method to a real trajectory.

4.3.1 Urban Transport Scenario

Tests were conducted along a track located within Calais city, France. Our test vehicle is equipped with a Novatel GPS receiver that calculates the position. The measurement campaign was conducted in an urban area during 5 minutes and 25 seconds. There are two areas where GPS positioning is absent due to an insufficient number of satellites: the first has duration of 40 seconds and the second 31 seconds. During these periods, the estimator uses odometer measurements which are delivered at a frequency of 1 Hz, as the GPS measurement when available. The test track is shown in figure 9.
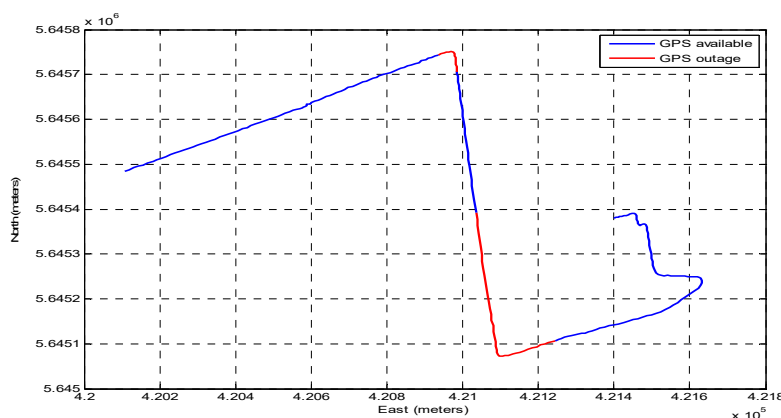

Figure 9. Real trajectory of the vehicle with long GPS outages

4.3.2 Vehicle Positioning

It is clear from figure 10 that the performance of the proposed method (gray rectangles) improves significantly the performance of the GPS/INS/Odometer integrated system with GPS outages (the rest of figure 10) in terms of velocity estimation. In fact, this method trusts the odometer measurements (East and North positions in addition to the heading angle) when GPS measures are not available and permits to readjust the INS navigation solution.
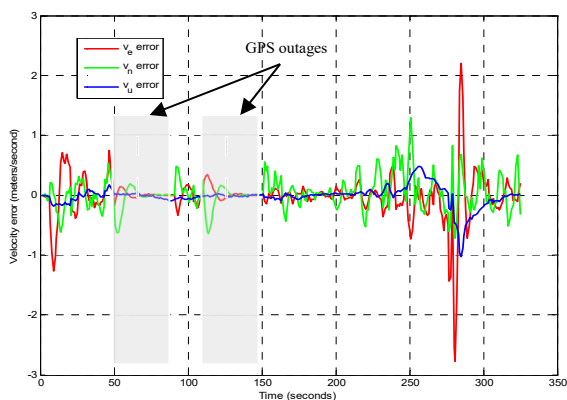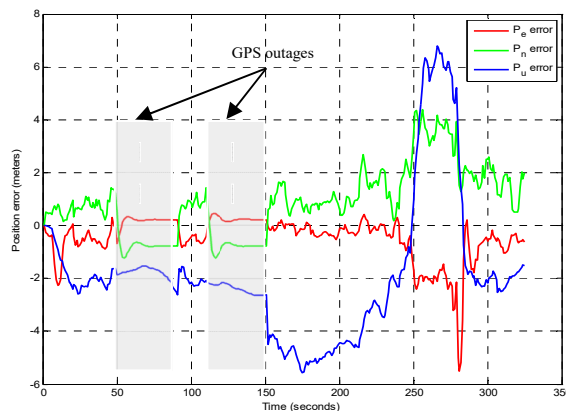
Figure 10. Velocity error of the vehicle

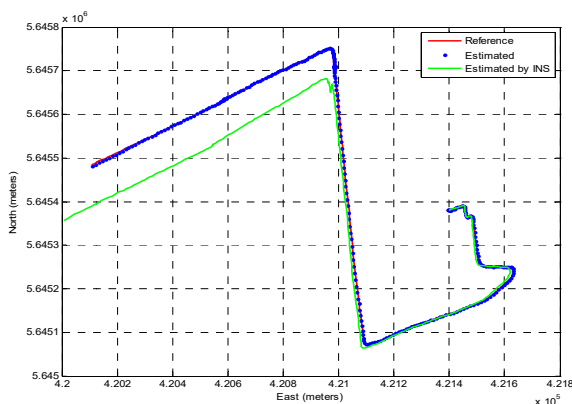Figure 11. Positioning error of the vehicle

Figure 12. The generated trajectory from
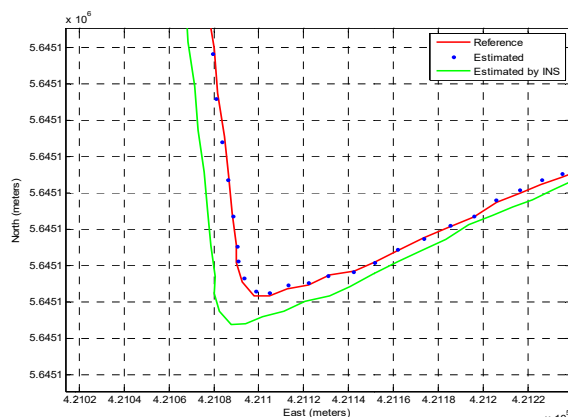GPS/INS/Odometer integrated navigation
system

Figure 13. Zoom on GPS/INS/Odometer
localization solution

Figure 11 shows the three-dimensional position estimation during GPS outages (gray rectangles) and in presence of GPS positioning (the rest of figure 11). As can be depicted from figure 11, the proposed method error estimates quickly converge to stable values after the initial transition period. The error doesn't exceed 1.5 meters for East and North components. Moreover, the points during GPS outages are selected to evaluate the localization accuracy of the proposed method. The table below presents the standard deviation of position error for both simulation data and real scenario during GPS outages, respectively. The table 1 shows that the new solution results are obviously better than the INS standalone system where GPS signals are absent; the standard deviation of the combined solution is 0.0217 meters and 0.2597 meters for both simulation and real data respectively. However, for standalone INS the standard deviation becomes 0.1437 meters and 1.1487 meters by the end of the vehicle trajectory.

Table 1. Position error standard deviation in meters

Data	GPS outages	
	INS only	INS and odometer
Simulation	0.1437	0.0217
Real	1.1487	0.2597

5. Conclusion

In summary, this paper proposes a new technique for GPS/INS/Odometer integration based on Kalman filter that minimizes the INS error and provides continuous estimation of vehicle position, velocity and attitude. This combination permit to avoid disadvantages of a stand-alone sensor in order to establish long-term navigation in GPS denied environments. The proposed method is a loosely-coupled solution that fuses the available measures. As described earlier the system presented in our work consists of the GPS receiver, an INS, and a vehicle odometer. The new technique solution was tested with real and simulated trajectories. The results for both trajectories were presented. The first trajectory contains 3 simulated GPS outages of 40 seconds duration were introduced intentionally. This was repeated four different. The proposed solution based on KF achieves centimeter-level positioning accuracy. The second trajectory is an urban scenario with natural GPS absence because of satellites signal blockage, where the proposed system solution was tested to demonstrate its performance in such environments.

In this work we have examined the odometer bridging performance for the Inertial Navigation System during GPS outages, and the results obtained from simulation and real tests confirm that using an additional aiding source, the odometer, provides more accurate navigation estimation than GPS/INS integrated system can offer in urban areas.

The proposed GPS/INS/Odometer integrated navigation system overcomes the problems due to environment of GPS signals propagation and shows good performance for land vehicle navigation solution using inertial sensors and an odometer in urban environment where the blockage of GPS satellites signals is very often.

References

Seo, J., & Lee, J. G. (2005). Application of nonlinear smoothing to integrated GPS/INS navigation system. *Journal of Global Positioning Systems, 4*(2), 88–94. http://dx.doi.org/10.5081/jgps.4.1.88

Noureldin, A., El-Shafie, A., & Taha, M. R. (2007). Optimizing neuro-fuzzy modules for data fusion of vehicular navigation systems using temporal cross-validation. *Engineering Applications of Artificial Intelligence, 20, pp.* 49–61. http://dx.doi.org/10.1016/j.engappai.2006.03.002

Farrell, J. (1998). *The Global Positioning System and Inertial Navigation*. McGraw-Hill Professional, New York.

Titterton, D. H., & Weston, J. L. (1996). *Strapdown Inertial Navigation Technology* (2nd Ed.). The American Institute of Aeronautics and Astronautics: Reston, VA, USA.

Wolf, R., Eissfeller, B., & Hein, G. (1997). A Kalman Filter for the Integration of a Low Cost INS and an attitude GPS. *In Proceedings of the International Symposium on Kinematic Systems in Geodesy, Geomatics and Navigation*, Banff, AB, Canada, pp. 143–150.

Solimeno, A. (2007). *Low-Cost INS/GPS Data Fusion with Extended Kalman Filter for Airborne Applications*. Master Thesis, Universidad Tecnica de Lisboa, Lisboa, Portugal.

Li, L., Wang, Y., Rizos, C., Mumford, P., & Ding, W. (2006). Low-Cost Tightly Coupled GPS/INS Integration Based on a Nonlinear Kalman Filtering Design. *In Proceedings of the 2006 National Technical Meeting of The Institute of Navigation*, Monterey, CA, USA, pp. 958–966.

Petovello, M. (2003). *Real-time Integration of a Tactical-Grade IMU and GPS for High-Accuracy Positioning and Navigation*. Ph.D. Thesis, Department of Geomatics Engineering, University of Calgary, Calgary, AB, Canada.

Babu, R., & Wang, J. (2007). Real-Time Data Analysis of Ultra-Tight GPS/INS. *In Proceedings of IGNSS Symposium 2007*, Sydney, NSW, Australia.

Pany, T., Kaniuth, R., & Eissfeller, B. (2005). Deep Integration of Navigation Solution and Signal Processing. *In Proceedings of the 18th International Technical Meeting of the Satellite Division of The Institute of Navigation* (ION GNSS 2005), Long Beach, CA, USA, pp. 1095–1102.

Petovello, M. G., & Lachapelle, G. (2006). Comparison of Vector-Based Software Receiver Implementations with Application to Ultra-Tight GPS/INS Integration. *In Proceedings of the 19th International Technical Meeting of the Satellite Division of The Institute of Navigation* (ION GNSS 2006), Fort Worth, TX, USA, pp. 1790–1799.

Jekeli, C. (2001). *Inertial navigation systems with geodetic applications*. Walter de Gruyter: Berlin, Germany.

Abd R. M., & El-Rabbany, A. (2015). Integration of GPS Precise Point Positioning and MEMS-Based INS Using Unscented Particle Filter. *Sensors, 15*(4), 7228-7245. http://dx.doi.org/10.3390/s150407228

Titterton, D., & Weston, J. L. (2004). *Strapdown Inertial Navigation Technology* (2nd Ed.). The American Institute of Aeronautics and Astronautics and the institution of electrical engineers: Reston, FL, USA.

Tang, J., Chen, Y., Niu, X., Wang, L., Chen, L., Liu, J., … Hyyppä, J. (2015). LiDAR Scan Matching Aided Inertial Navigation System in GNSS-Denied Environments. *Sensors*, *15* (7), 16710-16728. http://dx.doi.org/10.3390/s150716710

Angrisano, A. (2010). *GNSS/INS integration methods*. PhD thesis, Research in Geodetic Sciences and Topographic XXVIII Cycle, Department of Applied Sciences, University of Naples, Naples, Italy.

Schultz, C. E. (2006). *INS and GPS Integration*. M.Sc. Thesis, Technical University of Denmark, Kongens Lyngby, Denmark.

Quinchia, A. G., Falco, G., Falletti, E., Dovis, F., & Ferrer, C. (2013). A Comparison between Different Error Modeling of MEMS Applied to GPS/INS Integrated Systems. *Sensors*, *13*(8), 9549-9588. http://dx.doi.org/10.3390/s130809549

Abuhadrous, I. (2005). *Onboard real time system for 3D localization and modelling by multi-sensor data fusion*. domain other. Ecole Nationale Superieure des Mines de Paris, 62-64.

Lahrech, A., Boucher, C., & Noyer, J. C. (2005). Accurate vehicle positioning in urban areas. *Conference of the IEEE Industrial Electronics Society, 31.* http://dx.doi.org/10.1109/iecon.2005.1568953

Grewal, M. S., & Andrews, A. P. (1993). *Kalman Filtering: Theory and Practice*. Prentice-Hall, Inc.: Hoboken, NJ, USA.

Hou, H. (2004). *Modeling Inertial Sensors Errors Using Allan Variance*. The University of Galgary: Calgary, AB, Canada. UCGE Reports, No. 20201.

Shin, E. (2001). *Accuracy Improvement of Low Cost INS/GPS for Land Application*. MSc Thesis, Department of Geomatics Engineering, University of Calgary, Canada. UCGE Report, No. 20156.

Copyrights